**Third AO4ELT Conference - Adaptive Optics for Extremely Large Telescopes**
Florence, Italy. May 2013
ISBN: 978-88-908876-0-4
DOI: 10.12839/AO4ELT3.13438

# DISCRETE TIME $\mathbf{H}_\infty$ CONTROL OF TIP-TILT MODES WITH SATURATING ACTUATORS

Jean-Pierre Folcher[a]

UMR 7293 Lagrange - Université de Nice Sophia-Antipolis/CNRS/Observatoire de la Côte d'Azur, Parc Valrose, 06108 Nice cedex 2

**Abstract.** In the context of next generation instrumentation for current telescope and future Extremely Large Telescopes (ELT), the requirements on the correction of the tip-tilt modes are stringent. In a strong turbulence situation and in the presence of structural vibration of the telescope, tip-tilt mirror saturation phenomena can occur, which can degrade the performance or even destabilize the feedback system. In this paper a control method which ensures absolute stability against the mirror saturation is exposed. The proposed approach invokes the small gain theorem and is based on $H_\infty$ optimisation framework. The effectiveness of the proposed approach is demonstrated in a case study.

## 1 Introduction

It is well accepted that actuator saturation is present in practically all adaptive optics (AO) systems : physical constraints limit the amplitude of the control input signal. Actuator saturation can dramatically degrade the performance or even destabilize the closed-loop AO system. In many ways this phenomena is highly important for the tip-tilt correction. Atmospheric turbulence tip-tilt modes have a large amplitude and other effects (structural vibrations of the telescope, pre-focal mirror vibrations, telescope tracking error....) are added. In many AO systems, when the stroke of the deformable mirror is limited, the tip-tip modes are corrected by a specific tip-tilt mirror. In this paper we consider this specific feedback system where usually the saturation phenomena is implicitly taken into account. Numerous synthesis steps and extensive simulations are performed to check that the actuators never saturate. This approach involves numerous synthesis/validation steps and a limit of the controller gain is reached. By consequence poor closed loop performance is ensured. It is thus a "trial and error" approach which leads to prohibitive design time. In this paper we propose an alternative approach where the case of saturating actuators is considered. The design procedure guarantees absolute stability against the "excited" portion of the saturation and a certain level of closed loop performance.

## 2 Tip-tilt feedback system with saturating actuators

The tip-tilt controller has as input the measured output of the tip/tilt sensor (given by $y$) and provides a signal $u$ as control input. This signal $u$ is therefore sent to the actuators of the tip-tilt mirror which converts this low power signal to a higher power signal. The actuator saturation can be modeled by a linear system and a saturation function as depicted in figure 1. The actuator saturation can be described as

$$v = sat\,(u) \tag{1}$$

[a] folcher@unice.fr

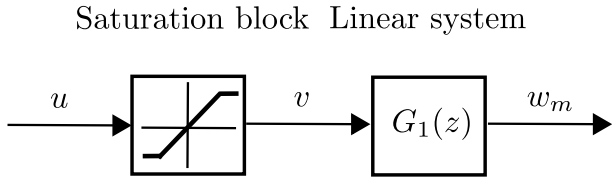


**Fig. 1.** Tip-tilt mirror model with saturation.

where *sat*(.) represents the saturation function defined by

$$\begin{aligned} sat(u) &= -u_{sat}, \quad u \leq -u_{sat}, \\ sat(u) &= u, \quad |u| \leq u_{sat}, \\ sat(u) &= u_{sat}, \quad u \geq u_{sat}. \end{aligned} \tag{2}$$

and where transfer function $G_1(z)$ is the linear part of the actuator. The saturation function and the feedback tip-tilt system are respectively depicted in figure 2 and 3. At each time instant k,

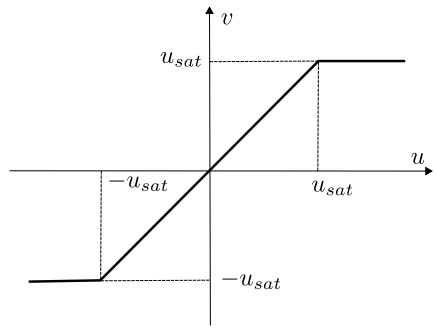


**Fig. 2.** The saturation function.

the atmospheric tip-tilt mode, the mirror shape tip-tilt correction and the residual tip-tilt error are described by discrete-time signals $w_a \in \mathbf{R}$, $w_m \in \mathbf{R}$ and $w_r \in \mathbf{R}$. The tip-tilt mirror is computer-controlled using control input signal $u \in \mathbf{R}$ and the tip-tilt sensor produces a discrete-time measurement $y \in \mathbf{R}$. The behavior of the tip-tilt mirror is determined by the function *sat*(.) and the transfer function $G_1(z)$. Furthermore, the tip-tilt sensor dynamic is described by the transfer function $G_2(z)$, the signal $n_w \in \mathbf{R}$ is an additive perturbation input of the measure $y$ and $K$ represents the controller transfer function.

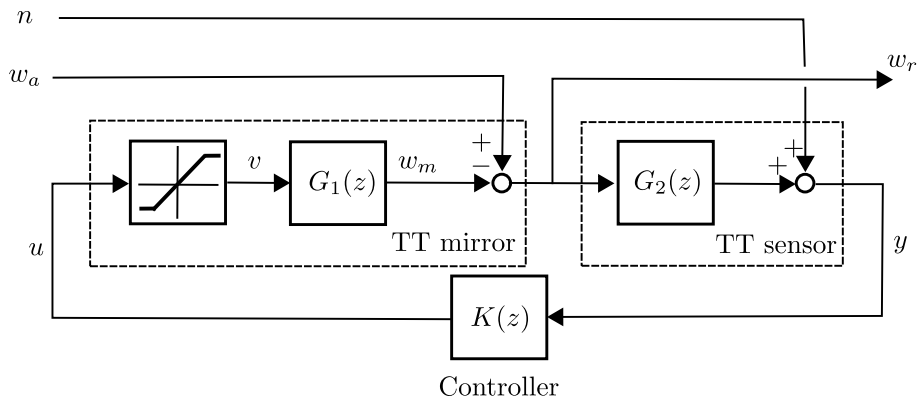


**Fig. 3.** Discrete time tip-tilt feedback system with saturating actuators.

We seek a controller $K(z)$ that garantees absolute stability against the "excited" portion of the saturation. Our methodology is based on the discrete-time version of the small gain theorem, see [5].

## 3 Stability analysis based on the small gain theorem

This approach studies the feedback connection of a linear dynamical system $H(z)$ and a nonlinear function $\Delta$, as shown in figure 4. The feedback connection $(H, \Delta)$ is stable if

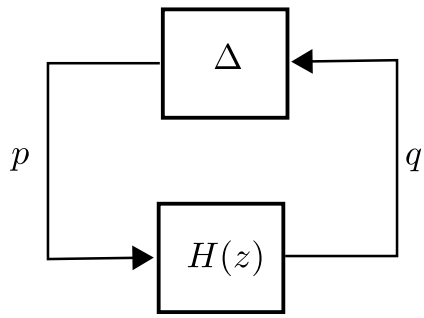


**Fig. 4.** Feedback connection of $(H, \Delta)$.

- the linear system $H(z)$ is asymptotically stable and

$$\|H(z)\|_\infty < \frac{1}{\beta} \text{ where } \|H(z)\|_\infty = \sup_{\Omega \in [0,2\pi]} \left|H(e^{j\Omega})\right| ,$$

- $\Delta$ is a norm-bounded (possibly time-varying) nonlinearity

$$|\Delta(u)| \leq \beta |u| \ .$$

Roughly speaking, the parameter $\beta$ is the "gain" of the nonlinear function $\Delta$. For high values of $\beta$, the feedback connection $(H, \Delta)$ is stable when the "gain" $\|H(z)\|_\infty$ of the linear system $H$ is small.

The saturation function $sat(u)$ is split into two parts : a linear function $\alpha u$ and a nonlinear function $\Delta(.)$, that is:

$$sat(u) = \alpha u - \Delta(u)$$

where $\alpha$ is a given parameter. Then, the tip-tilt feedback system depicted in figure 3 is rearranged to form an equivalent feedback system shown in figure 5. The linear system output signal denoted $q$ is $q = u$, the linear system input signal $p$ is equal $p = \Delta(q)$ and we write Eq. 1 as $v = \alpha u - p$. This equivalent feedback system can be seen as the $(H, \Delta)$ connection: the output signal $q$ depends on input signal $p$ through the transfer function $H(z)$ where exogenous signals $n$ and $w_a$ are assumed to be zero. To make this explicit,

$$\mathcal{Z}\{q\} = \underbrace{\frac{K(z)G_1(z)G_2(z)}{1 + \alpha K(z)G_1(z)G_2(z)}}_{H(z)} \mathcal{Z}\{p\}$$

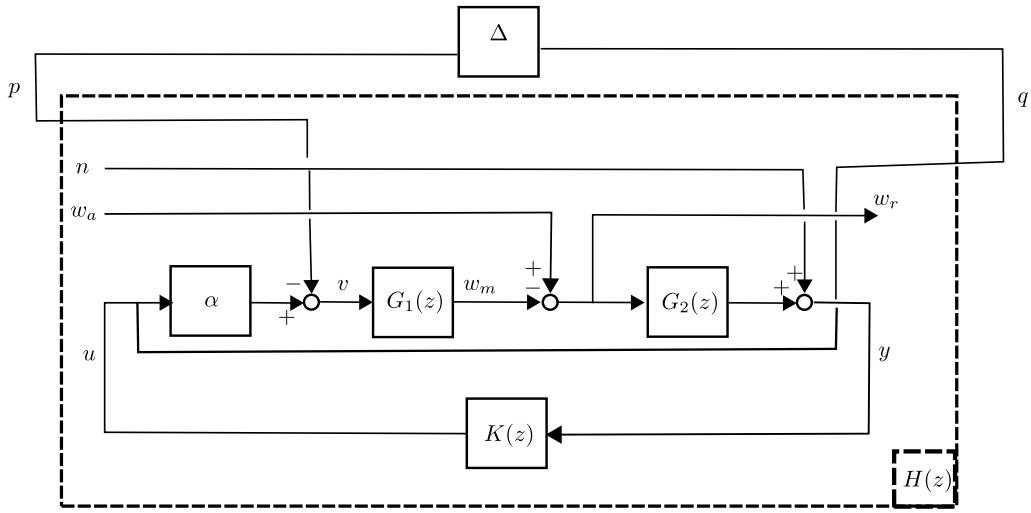


**Fig. 5.** Equivalent feedback system.

For the set of exogenous input $w_a$ and $n_w$, we assume that the modulus of the control input signal $u$ is bounded, that is

$$-u_{max} \leq u(k) \leq -u_{max}$$

where $u_{max}$ is a design parameter with $u_{max} \geq u_{sat}$. Thus, from the definition of the saturation function given in Eq. 2, it is easy to show that $\Delta$ is a norm-bounded (possibly time-varying) nonlinearity where

$$\alpha = \frac{u_{max} + u_{sat}}{2u_{max}}, \quad \beta = \frac{u_{max} - u_{sat}}{2u_{max}} .$$

Using the small gain theorem, the stability is ensured when

$$\left\| \frac{K(z)G_1(z)G_2(z)}{1 + \alpha K(z)G_1(z)G_2(z)} \right\|_\infty < \frac{2u_{max}}{u_{max} - u_{sat}} . \tag{3}$$

## 4 $H_\infty$ tip-tilt controller design

The standard $H_\infty$ framework is represented in figure 6. In this figure, $w$ is the exogenous input (reference, perturbation, noise,...). The control input is $u$, $z$ is the regulated output, and $y$ is the measure. $P(z)$ is the generalized plant and $K(z)$ is the controller. Let $T_{zw}(z)$ be the transfer matrix

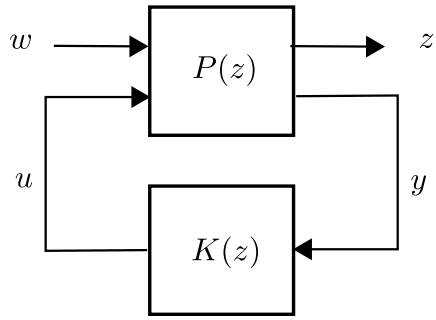


**Fig. 6.** $H_\infty$ framework.

between regulated output $z$ and the exogenous input $w$. The control objectives are defined as

- the feedback system is stable,
- the $\mathbf{H}_\infty$ norm between the input $w$ and the output $z$ is bounded

$$\|T_{zw}(z)\|_\infty = \sup_{\Omega\in[0,2\pi]} \bar{\sigma}\left(T(e^{j\Omega})\right) < \gamma \ .$$

This problem is the so-called standard $H_\infty$ control problem and lead to the resolution of algebraic Riccati equations [2,6]. This problem can also be reformulated as an optimization problem involving linear matrix inequalities (LMIs), see [3].

A convenient synthesis framework is illustrated in figure 7 where the linear part of the equivalent feedback system depicted in figure 5 is re-arranged to form what is called the synthesis framework. Transfer function $W_1(z)$ and $W_2(z)$ are added to take into account the spectral content of the atmospheric mode $w_a$ and the tip-tilt sensor noise $n$. Transfer function $W_3(z)$ is introduced to penalize control input $u$.

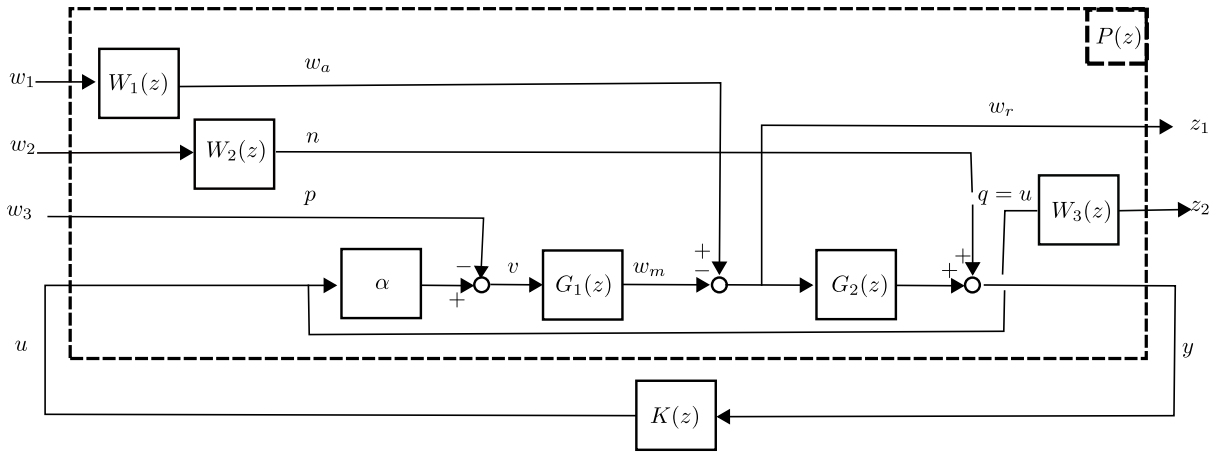


**Fig. 7.** Synthesis framework.

We can recognize the standard $H_\infty$ block diagram shown in figure 6. Therefore, the $H_\infty$ design ensures that the $H_\infty$-norm of transfer matrix $T_{zw}(z)$ is bounded by $\gamma$:

$$\begin{aligned}\|T_{zw}(z)\|_\infty &= \left\| \begin{matrix} T_{z_1w_1}(z) & T_{z_1w_2}(z) & T_{z_1w_3}(z) \\ T_{z_2w_1}(z) & T_{z_2w_2}(z) & T_{z_2w_3}(z) \end{matrix} \right\|_\infty , \\ &= \left\| \begin{matrix} W_1(z)T_{w_rw_a}(z) & W_2(z)T_{w_rn}(z) & T_{w_rp}(z) \\ W_1(z)W_3(z)T_{uw_a}(z) & W_2(z)W_3(z)T_{un}(z) & W_3(z)T_{up}(z) \end{matrix} \right\|_\infty < \gamma.\end{aligned}$$

If the previous inequality is enforced, then every block of the transfer matrix $T_{zw}(z)$ has an $H_\infty$-norm bounded by $\gamma$. For instance,

$$\left\|W_1(z)T_{w_rw_a}(z)\right\|_\infty < \gamma \text{ is equivalent to } \forall\omega, \ \left|W_1(e^{j\omega T})T_{w_rw_a}(e^{j\omega T})\right| < \gamma$$

and we obtain

$$\forall\omega, \ \left|T_{w_rw_a}(e^{j\omega T})\right| < \frac{\gamma}{\left|W_1(e^{j\omega T})\right|} \ .$$

Likewise

$$\left|T_{w_r n}(e^{j\omega T})\right| < \frac{\gamma}{\left|W_2(e^{j\omega T})\right|}\ , \quad \left|T_{w_r n}(e^{j\omega T})\right| < \gamma\ , \quad \left|T_{u w_a}(e^{j\omega T})\right| < \frac{\gamma}{\left|W_1(e^{j\omega T})\right|\left|W_3(e^{j\omega T})\right|}\ ,$$

$$\left|T_{un}(e^{j\omega T})\right| < \frac{\gamma}{\left|W_2(e^{j\omega T})\right|\left|W_3(e^{j\omega T})\right|}\ , \quad \left|T_{up}(e^{j\omega T})\right| < \frac{\gamma}{\left|W_3(e^{j\omega T})\right|}\ .$$

## 5 Sample numerical results

The main features of the proposed design approach are presented in this section for a representative model of a tip-tilt stage. The block diagram of this tip-tip feedback system is depicted in figure 3 where the control input signal $u$ has the same units than the resigual error signal $w_r$, expressed in milliarseconds $[arcsec]$. The tip-tilt mirror dynamics is assumed to be a second-order model where the damping factor is $\zeta = 0.4$, the natural frequency is $\omega_n = 660\ rd/s$ and the DC gain is unitary. The considered saturation level is given by $u_{sat} = 1.9$. The tip-tilt sensor is a four quadrant detector operating at $1\ 500\ Hz$. The discrete-time transfer functions $G_1(z)$ and $G_2(z)$ incorporate the effects of the mirror dynamic model, the zero-order hold, the frame integration and the computation time of the control input. These transfer functions are computed using the method presented in [9]

$$G_1(z) = 2.93\ 10^2 \frac{(z + 3.3878)(z + 0.2474)}{z(z^2 - 1.5427z + 0.7033)}, \quad G_2 z(z) = \frac{7.37}{z}\ .$$

For the purposes of the case study, we consider a tip-tilt time sequence $w_a$ derived from phycically simulations for a telescope where the pupil diameter is $D = 1.52m$, and the obstruction ratio is $r = 0.3$. The parameters of the optical turbulence in the atmosphere are : (i) a Fried parameter $r_0 = 10\ cm$ for $\lambda = 600\ \eta m$ ; (ii) an outer scale of 25 m ; (iii) wind velocities ranging from 8 $m/s$ to 12 $m/s$.

The controller design was performed using the approach exposed in section 4 where we assume that the control input is bounded by $u_{max} = 3.2$. The feedback performance is fixed by the choice of the following weighting functions

$$W_1(z) = 0.60\ \frac{z - 0.6667}{z - 1}, \quad W_2(z) = 157.64\ \frac{z - 0.8750}{z + 0.9704},$$

$$W_3(z) = 16.67\ \frac{(z - 1)(z - 0.8182)}{(z + 0.8182)(z - 0.6667)}.$$

They are obtained by converting continuous time weighting function which are easier to tune using the Tustin transform. The smallest $\gamma$ achieved for was $\gamma = 3.005$. The designed controller has five extra poles which are not necessary to control the system. These extra poles are removed using controller reduction method and we obtain the third order transfer function

$$K(z) = 1.31\ 10^{-3}\ \frac{(z + 1)^3}{(z - 1)(z - 0.0176)(z + 0.0148)}.$$

Figure 8(a) shows the Bode diagram of the sensitivity transfer function $T_{w_r w_a}(z)$ and the template $\gamma W_1^{-1}(z)$. The weighting function shapes the frequency response in the low frequency domain and ensures a correct modulus margin and a bandwith of 630 $rad/s$. The frequency response of

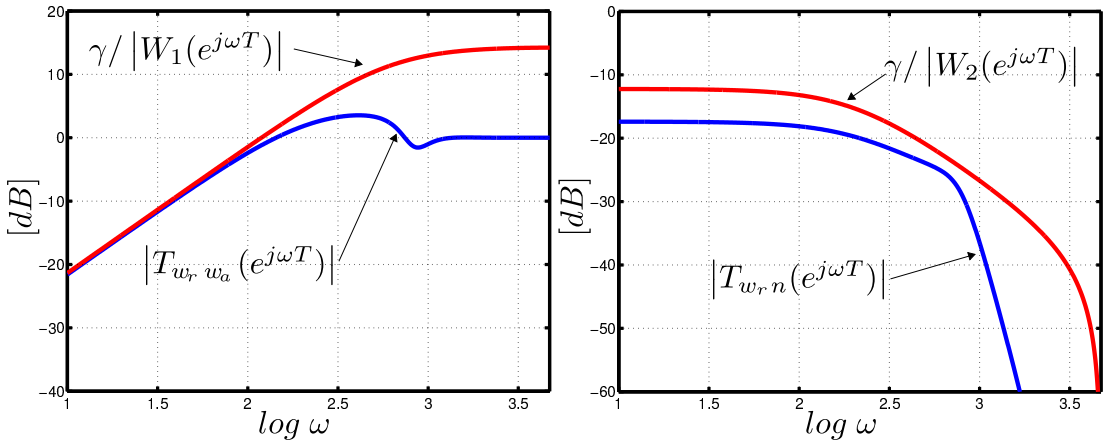


**Fig. 8.** Bode plot of the sensitivity transfer function $T_{w_r w_a}(z)$ in the left part, and Bode plot of the noise transfer function $T_{w_r n}(z)$ in the right part.

the closed loop transfer function $T_{w_r n}(z)$ and of the template $\gamma W_2^{-1}(z)$ are plotted in figure 8(b). Note that the weighting function shapes the frequency response in the high frequency domain to reject the sensor noise contribution. Figure 9(a) shows the Bode diagram of the sensitivity transfer function $T_{uw_a}(z)$ and the template $\gamma W_3^{-1}(z)$. The weighting function shapes the frequency response in the high frequency domain to ensure reasonable values of control input. The frequency response of the closed loop transfer function $T_{up}(z)$ is plotted in figure 9(b). We can check that the condition given in Eq.3 holds and thus the feedback system stability is ensured. Figure 10 shows the closed loop time response for a given atmospheric disturbance time se-

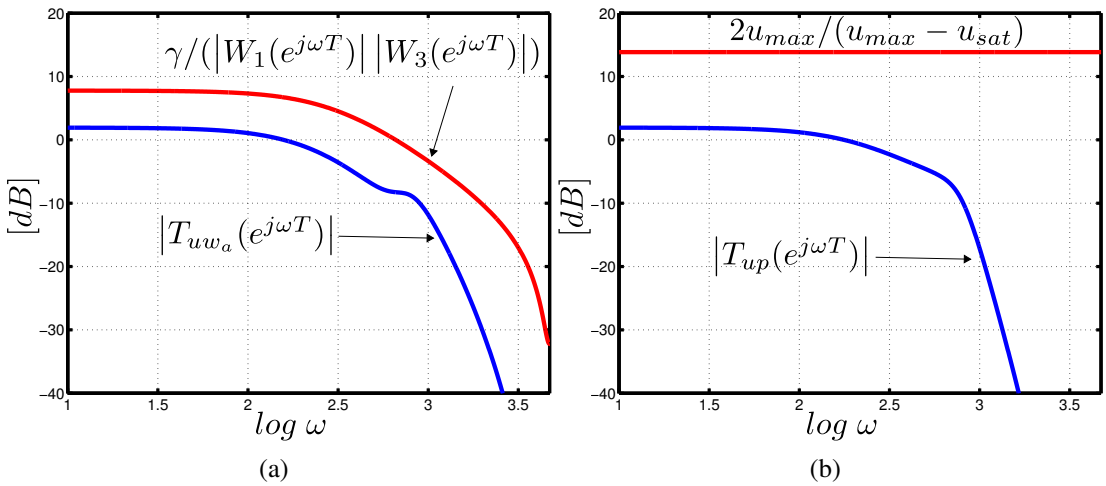


**Fig. 9.** Bode plot of sensitivity transfer function $T_{w_r w_a}(z)$ in the left part, and Bode plot of transfer function $T_{up}(z)$ in the right part.

quence. The tip-tilt mirror correction is efficient and remark that when the mirror saturates the feedback system stability is not lost. In conclusion, the proposed approach based on $H_\infty$ optimization provides a computationally simple way of designing controllers for systems with saturating actuators and guarantees the closed loop stability for a given level of saturation $u_{max}$.

.

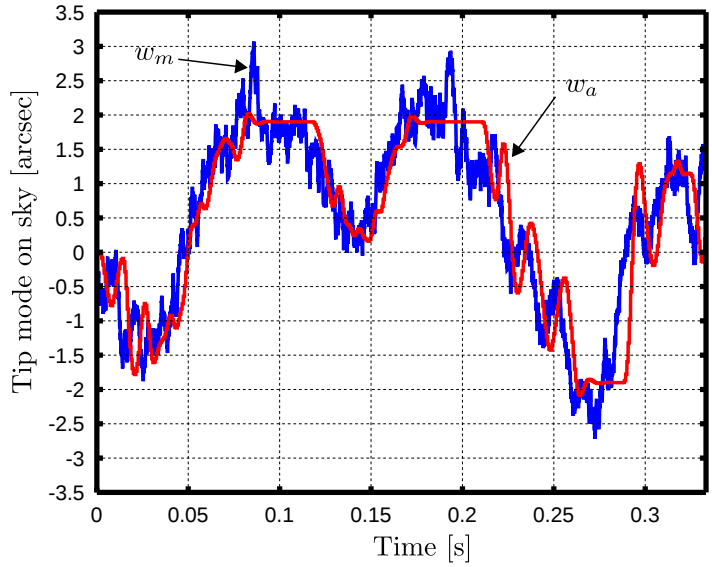


**Fig. 10.** Time evolution for the atmospheric disturbance $w_a$ (plotted in blue) and tip-tilt mirror correction $w_m$ (plotted in red).

## References

1. N. Denis, D. Looze, J. Huang, and D. Castañon. Kybernetika **35(1)**, (1999) 69.
2. J. Doyle, K. Glover, P. P. Khargonekar, and B. A. Francis. TAC **34(8)**, (1989) 831.
3. P. Gahinet and P. Apkarian. IJNRC **4(4)**, (1994) 421.
4. A. Guesalaga, B. Neichel, J. O'Neal, and D. Guzman. Optics Express **21(9)**, (2013) 10676.
5. W. Haddad and D. Bernstein. IJNRC **4(2)**, (1994) 249–265.
6. P. Iglesias and K. Glover. IJNRC **54(5)**, (1991) 1031.
7. C. Kulcsár, H.-F. Raynaud, C. Petit, and J.-M.Conan. Proc. Opt. Soc. Am., OSA, (2007).
8. C. Kulcsár, H.-F. Raynaud, C. Petit, and J.-M.Conan. SPIE Proc. **7015**, (2008) 70151G.
9. D.P. Looze. Automatica **41(11)**, (2005) 2005.